Atom Transfer Radical Polymerization of Methylmethacrylate and Styrene Initiated by 3,5-bis(perfluorobenzyloxy)benzyl 2-Bromopropanoate

Tuba Çakır Çanak, Mukaddes Selçukoğlu, Esin Hamuryudan, İ. Ersin Serhatlı

Department of Chemistry, Istanbul Technical University, Maslak 34469, Istanbul, Turkey

ABSTRACT: The synthesis of polymethylmethacrylate (pMMA) and polystyrene (pSt) were realized with newly synthesized initiator, 3,5-bis(perfluorobenzyloxy)benzyl 2-bromopropanoate (FBr) in the presence of copper bromide (CuBr) and N,N,N',N'',N''-pentamethyl-diethyl-enetriamine (PMDETA) by using atom transfer radical polymerization (ATRP). The perfluorinated aromatic group containing initiator was prepared by esterification of the (3,5-bis[(perfluorobenzyl)oxy]-phenyl alcohol. Both initiator and polymers were characterized by ^{1}H-NMR spectroscopy, gel permeation chromatography, differential scanning calorimetry, and thermogravimetric analysis. The ATRP was supported by an increase in the molecular weight of the forming polymers and also by their monomodal molecular weight distribution. Contact angle measurements of water and ethylene glycol on films of synthesized polymers indicated higher degree of hydrophobicity than that of pure pMMA and pure pSt. © 2011 Wiley Periodicals, Inc. J Appl Polym Sci 124: 1683–1694, 2012

Key words: ATRP; polymethylmethacrylate; polystyrene; fluorinated polymers; initiator

INTRODUCTION

Fluorinated polymer films exhibit excellent barrier properties[1] and extremely low critical surface tensions,[2] causing water and oils to bead up on surface. Fluorocarbon compounds have unique properties quite different from those of their hydrocarbon counterparts. Small amounts of fluorocarbon additives significantly reduce the surface energy of conventional hydrocarbon-based polymers to change the surface properties exhibiting extremely high hydrophobic and lipophobic characters. However, their use is very limited by incompatibility of fluorocarbons with nonfluorinated conventional polymers. To overcome this problem, fluorocarbon compounds are attached to the polymer chain ends to prepare block copolymers containing fluorinated blocks and chain-end-functionalized polymers with one fluorocarbon moiety.

The fluorine can be incorporated into the main polymer chain. Examples using fluorinated diols[3–5] and fluorinated alcohols[6] to prepare polyurethanes have been reported. Surface energy reduction has also been studied using blends of fluoropolymers with hydrocarbon polymers.[7,8] Several reports have used the propensity of chain-end enrichment at surfaces in conjunction with fluorination to alter surface energies.[9–14] Surface tension reduction has also been reported for copolymers prepared by the incorporation of fluorinated monomers and by chemically grafting perfluoroalkyl groups to polymers.[15–18]

Living/controlled polymerizations of fluorinated monomers are essential to the design and practical synthesis of fluorinated polymers with well-defined architectures. Several methods of living/controlled radical polymerization have been developed in the past decade. Atom transfer radical polymerization (ATRP)[19–22] is one of the most promising system and has attracted wide research interests.[23–34] It has proven to be efficient for a wide range of monomers (styrenes, meth(acrylates), acrylonitriles, etc.),[27] polymerizing not only with Cu catalyst but with transition-metal complexes of Ru,[35] Pd,[36] Ni,[37] and Fe.[38–41] Polymerization is conducted either in bulk or in other solvents (benzene, water, etc.).[42,43] It is generally performed at moderate temperatures (70–130°C). For all these reasons, ATRP has become a powerful tool for academic as well as industrial polymer chemists, allowing efficient synthesis of novel, tailor-made materials.[27,28] One of the most attractive features of ATRP is the preparation of many new functional polymers with novel and controlled compositions and topologies for structure-property relationship,

and the better design of novel materials for special applications. This method is especially well suited for that purpose as a result of facile conditions, a multitude of polymerizable monomers, and accessible chain functionalities.

ATRP using fluorine-functionalized initiators is a convenient procedure for the synthesis of chain-end-functionalized polymers with fluorine groups.[44–50] Destarac et al.[45] synthesized several interesting polymers chain-end-functionalized with fluorine groups by Cu-mediated ATRP initiated with CCl_3-terminated vinylidene fluoride (VF) telomers. Similarly, CCl_3-terminated co-telomer of VF and hexafluoropropylene was used as an initiator in the ATRP of MMA.[46] 2-Perfluoroalkyl ethyl 2-bromoisobutyrate, its derivatives, and (perfluorononenyloxy)benzenesulfonyl chloride are also suitable initiators for the same synthetic purpose.[47–50]

Like fluorinated block copolymers, even one fluorocarbon moiety attached to the polymer chain end significantly influences properties and behavior of air–water, air–polymer, polymer–polymer surfaces, and interfaces. In fact, many research groups have reported that chain-end-functionalization of polymers with the fluorine group can dramatically change the surface and solution properties by surface segregation, formation of micelles, etc.[51] So, the purpose of this study is to prepare chain-end fluorinated polymers and to investigate the effect of this fluorine group to the polymer surface and thermal properties. For this, a novel fluorinated ATRP initiator was synthesized and used for the polymerization of styrene and methylmethacrylate. The efficiency of the synthesized initiator is evaluated and discussed on the basis of the molecular weight and polydispersity of the polymers. Synthesized initiator was characterized by Fourier transform infrared spectroscopy (FTIR), ^{19}F-NMR, and ^{1}H-NMR. Obtained fluorine end-capped polymers were also characterized by ^{1}H-NMR, gel permeation chromatography (GPC), and the thermal properties were examined by differential scanning calorimetry (DSC) and thermogravimetric analysis (TGA) methods. Thin films of these polymers were prepared by spin coating to investigate the wetting behavior of the polymers and surface contact angle values were measured.

EXPERIMENTAL

Materials

St (Fluka), MMA (Fluka) were purified by conventional methods and distilled *in vacuo* over CaH_2 just before use. Tetrahydrofuran (J. T. Baker) was dried over potassium hydroxide and distilled over CaH_2. Other chemicals, *N,N,N′,N″,N″-pentamethyl-diethyl*-diethylenetriamine (PMDETA) (97% Aldrich), copper (I) bromide (98% Aldrich), anisole (99% Acros), triethylamine (99% Acros), 2-bromoproionyl bromide (97% Aldrich), pentafluorobenzyl bromide (98% Alfa Aesar), 3,5-dihydroxybenzyl alcohol (99% Aldrich), and 18-crown-6 (Merck, 99%) were used without further purification.

Characterization and analysis

FTIR spectra was measured using model recorded Perkin-Elmer Spectrum One FTIR (ATR sampling accessory) Spectrophotometer. ^{1}H-NMR and ^{19}F-NMR spectra were determined on Bruker AC spectrometer at 250 MHz and Varian Inova spectrometer at 500 MHz, respectively, using $CDCl_3$ as solvent. Chemical shifts were reported in ppm from internal tetramethylsilane (TMS) (^{1}H-NMR) or from internal $CFCl_3$ (^{19}F-NMR). GPC analyses were performed with a set up consisting of the Agilent pump and refractive-index detector and three Agilent Zorbax PSM 1000S, 300S, and 60S columns (6.2×250 mm, 5 micron) measuring in the range of 10^4–10^6, 3×10^3–3×10^5, 5×10^2–10^4, respectively. Tetrahydrofuran (THF) was used as the eluent at a flow rate of 0.5 mL/min at 30°C. The molecular weights (MWs) of the polymers were calculated with the aid of polystyrene (pSt) standards. The thermal properties of the polymers were measured by differential scanning calorimeters (TA, DSC Q10) in a flowing nitrogen atmosphere from 30°C at scanning rate of 10°C/min. Thermal stability of copolymers was measured by thermo gravimetric analysis (TA, TGA Q50) in a flowing nitrogen atmosphere at heating rate of 20°C/min. Contact angle measurements and surface free energy calculations were performed using KSV Attension Theta Lite contact angle instrument; deionized water and ethylene glycol drops (4–8 μL) were dispensed from a 1000 μL syringe. Contact angle measurements were reported as an average of three areas on different portions of the film surface. In this study, geometric-mean approximations were used to obtain the dispersive and nondispersive contributions to the total surface energy.

According to Owens and Wendt,[52] the surface energy of a given solid can be determined using an equation applied to two liquids.

Synthesis of 3,5-bis[(pentafluorobenzyl)oxy]benzyl alcohol

K_2CO_3 (3.52 g, 25.4 mmol) and 18-crown-6 (0.32 g, 1.21 mmol) were added, respectively, into a mixture of pentafluorobenzyl bromide (6.62 g, 25,3 mmol) and 3,5-dihydroxybenzyl alcohol (1,71 g, 12.2 mmol) in acetone (100 mL) at room temperature and allowed to stir vigorously under nitrogen. After 3 days, the solvent was removed *in vacuo*, the residue was partitioned between water (20 mL) and CH_2Cl_2 (20 mL), the aqueous layer was extracted with CH_2Cl_2 (3 × 200 mL), and the CH_2Cl_2 extracts were
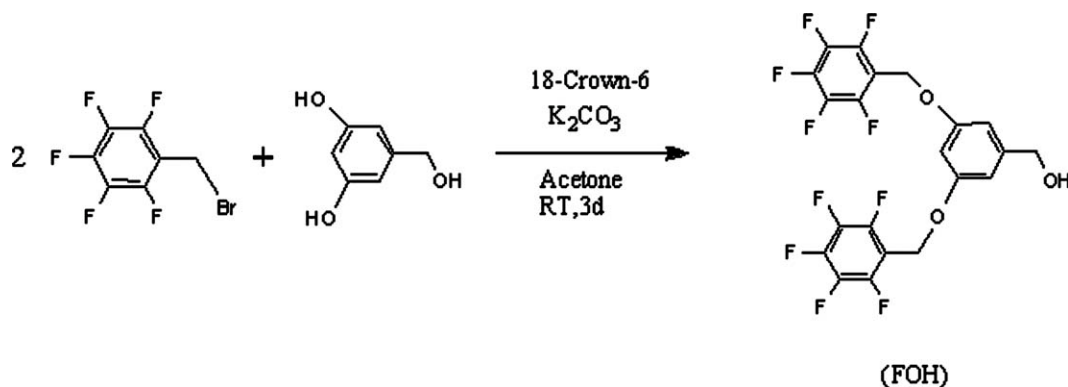
Scheme 1 Synthesis of FOH.

combined, dried over MgSO₄, and concentrated *in vacuo*. The product, 3,5-bis[(pentafluorobenzyl)oxy]-benzyl alcohol (FOH), was obtained by crystallization from 50% hexane/CH₂Cl₂. Yield = 61% T_m = 98°C; FTIR ν (cm⁻¹) : 3294, 2897, 1659, 1597, 1525, 1453, 1376, 1280, 1125, 930, 826, 769, 688; ¹H-NMR (CDCl₃) δ = 2.16 (t, 1H), 4.66 (d, 2H), 5.10 (s, 4H), 6.47 (t,1H), 6.64 (d, 2H) ppm; ¹⁹F-NMR (CDCl₃) δ = −145.2 (m, 4F, *ortho-F*), −155.4 (m, 2F, *para-F*), −164.5 (m, 4F, *meta-F*) ppm.

Synthesis of 3,5-bis(perfluorobenzyloxy)benzyl 2-bromopropanoate

Under nitrogen 0.55 mL (5.25 mmol) 2-bromopropionyl bromide was added dropwise to a stirring mixture of 3,5-bis[(perfluorobenzyl)oxy]-benzyl alcohol (FOH) (2.12 g, 4.12 mmol) and triethylamine (0.72 mL, 5.13 mmol) in 10 mL of THF in an ice bath for 1 h. After complete addition of the acid bromide, the reaction was stirred at room temperature for 3 h. The reaction mixture was washed with water (3 × 30 mL) and then dried over MgSO₄. After filtration and evaporation of THF, a greasy white product was obtained. It was dried under vacuum and recrystallized from ethanol. m.p: 68°C, Yield: 59%. FTIR ν (cm⁻¹): 2918, 1737, 1653, 1597, 1322, 1161, 930, 847, 716; ¹H-NMR (CDCl₃), δ (ppm): 6.6 (m,

2H), 6.5 (m,1H), 5.2 (m,2H), 5.1 (m,4H), 4.5 (q,1H), 1.7–1.9 (d,3H). ¹⁹F-NMR (CDCl₃) δ = −145.1 (m, 4F), −155.3 (m, 2F), −164.4 (m, 4F) ppm.

Synthesis of fluorinated pSt and polymethylmethacrylate

To a schlenk tube equipped with a magnetic stirrer, vacuum and dry nitrogen was applied three or four times, then certain amounts of monomer (St or MMA), anisole, CuBr, PMDETA, and initiator (FBr) were added in the order mentioned under nitrogen. The reaction solution was bubbled by nitrogen to remove dissolved gases, and then, tube was immersed in an oil bath and held by a thermostate at 90 or 95°C, with rigorous stirring. At each interval, a 1.0 mL sample was taken from the flask with a degassed syringe to trace the course of the polymerization. The polymerization was performed for a determined time. Then, the tube was cooled to room temperature, and the contents were dissolved in large amount of THF. The THF solution was passed through a short neutral alumina column to remove copper complex and then excess THF was removed by evaporation. The polymer was precipitated into excess methanole, isolated by vacuum filtration and dried at room temperature *in vacuo*. The conversion was determined gravimetrically.
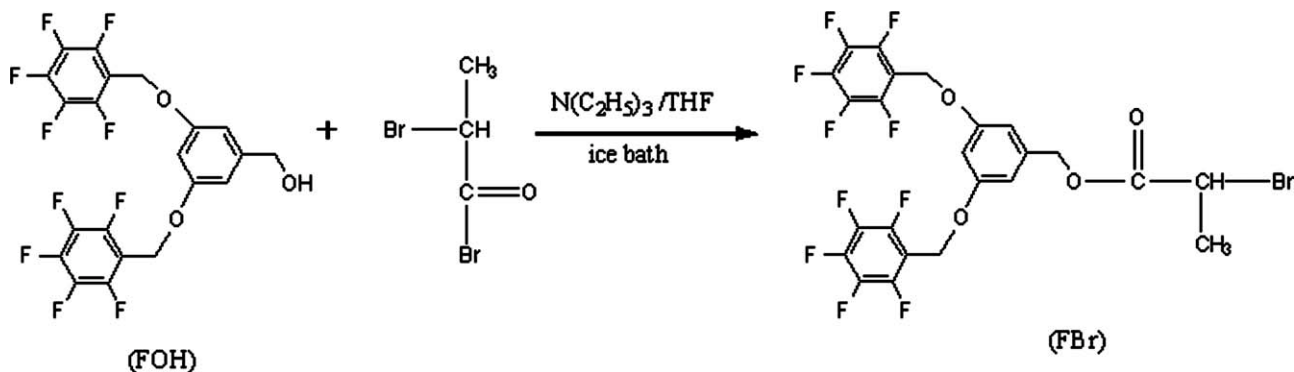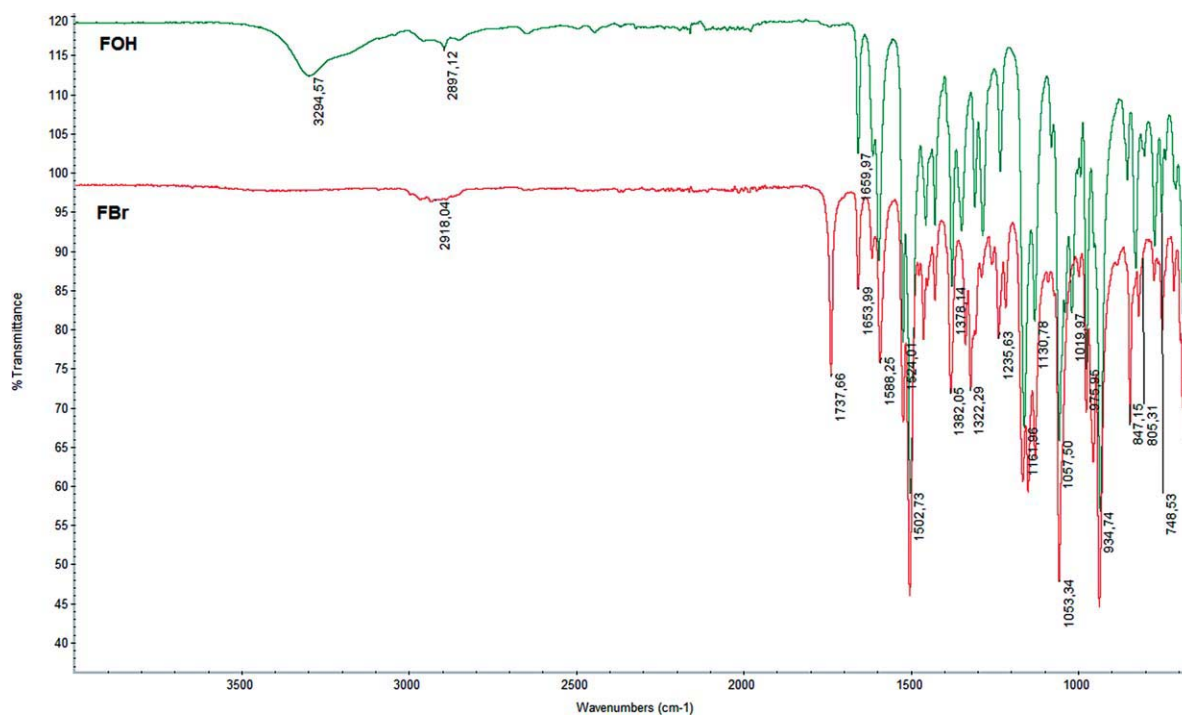

Scheme 2 Synthesis of FBr.

Figure 1 FTIR spectrum of FOH and FBr [Color figure can be viewed in the online issue, which is available at wileyonlinelibrary.com].

Film preparation

Thin polymer films were spin-coated (1000 rpm for 30 s) using a SCS P6700 spin coater onto a clean and dried glass substrate using solutions of the synthesized polymers with concentrations of 100 mg in 1 mL of toluene. After spin-coating, the polymer films were annealed for 2 h at 125°C in an oven. By

this procedure, glass substrate was completely covered with the polymers.

RESULTS AND DISCUSSION

In this study, perfluoroaromatic group end-capped pSt and polymethylmethacrylate (pMMA) were
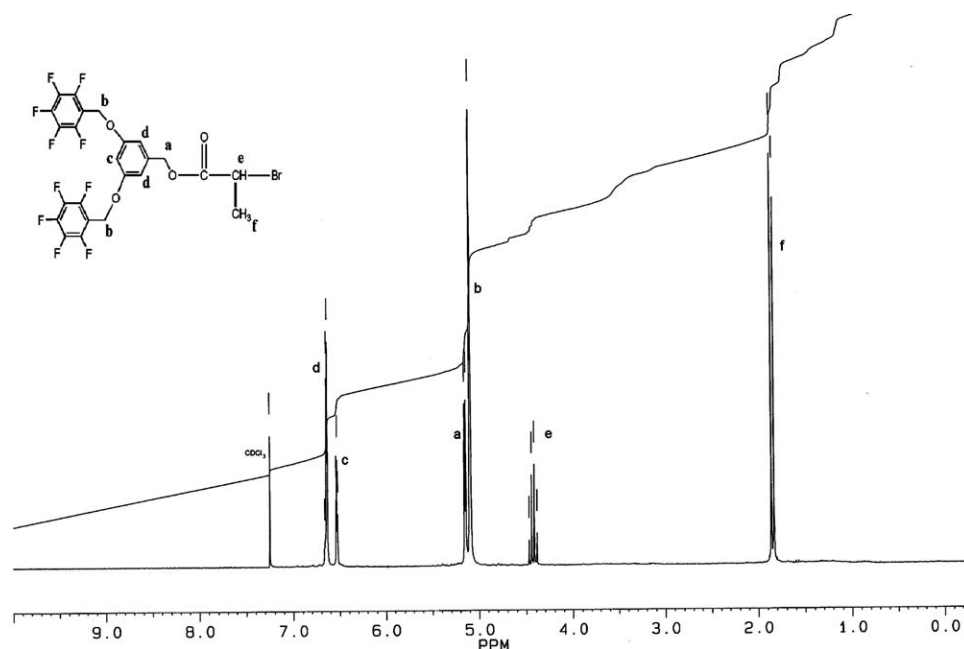

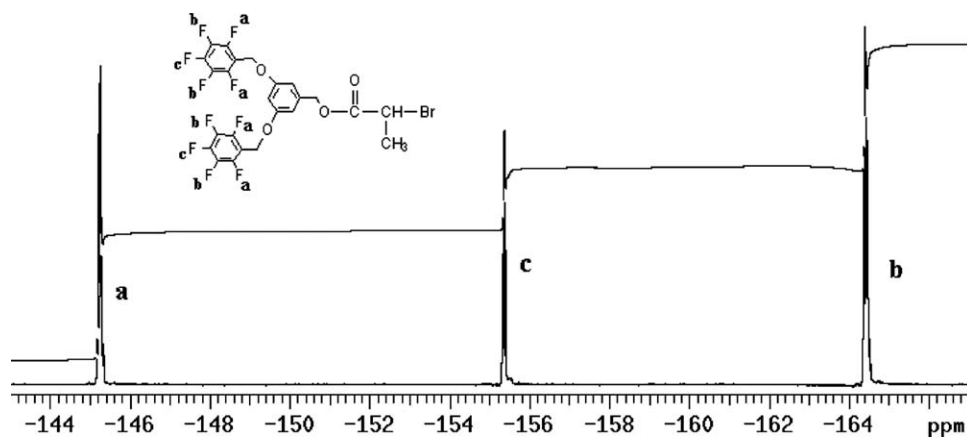**Figure 2** ¹H-NMR (in CDCl₃) spectrum of FBr.

Figure 3 ^{19}F-NMR (in CDCl$_3$) spectrum of FBr.

synthesized via ATRP technique. For this purpose, 3,5-bis[(perfluorobenzyl)oxy]-benzyl alcohol (FOH) was used for the preparation of FBr. Reaction of 3,5-dihydroxybenzyl alcohol with α-bromopentafluoro-toluene, in the presence of K$_2$CO$_3$ and 18-crown-6, in acetone at room temperature for 3 days gave FOH in 61% yield. (Scheme 1). Then perfluorinated aromatic group containing ATRP initiator was synthesized by esterification of the FOH with 2-bromo-propionylbromide (Scheme 2).

The structure of the product FBr was confirmed by spectroscopic investigations. The FTIR spectrum showed no signal corresponding to —OH groups of the starting FOH at 3294 cm^{-1} and shows the characteristic C=O ester band at 1737 cm^{-1} and C—Br band at 688 cm^{-1} (Fig. 1). ^{1}H-NMR spectrum recorded in CDCl$_3$ evidenced resonance signals of —CH$_3$, —CH$_2$, —OCH$_2$, and —CH—Br protons of relative intensities corresponding to the number and type of protons (Fig. 2).
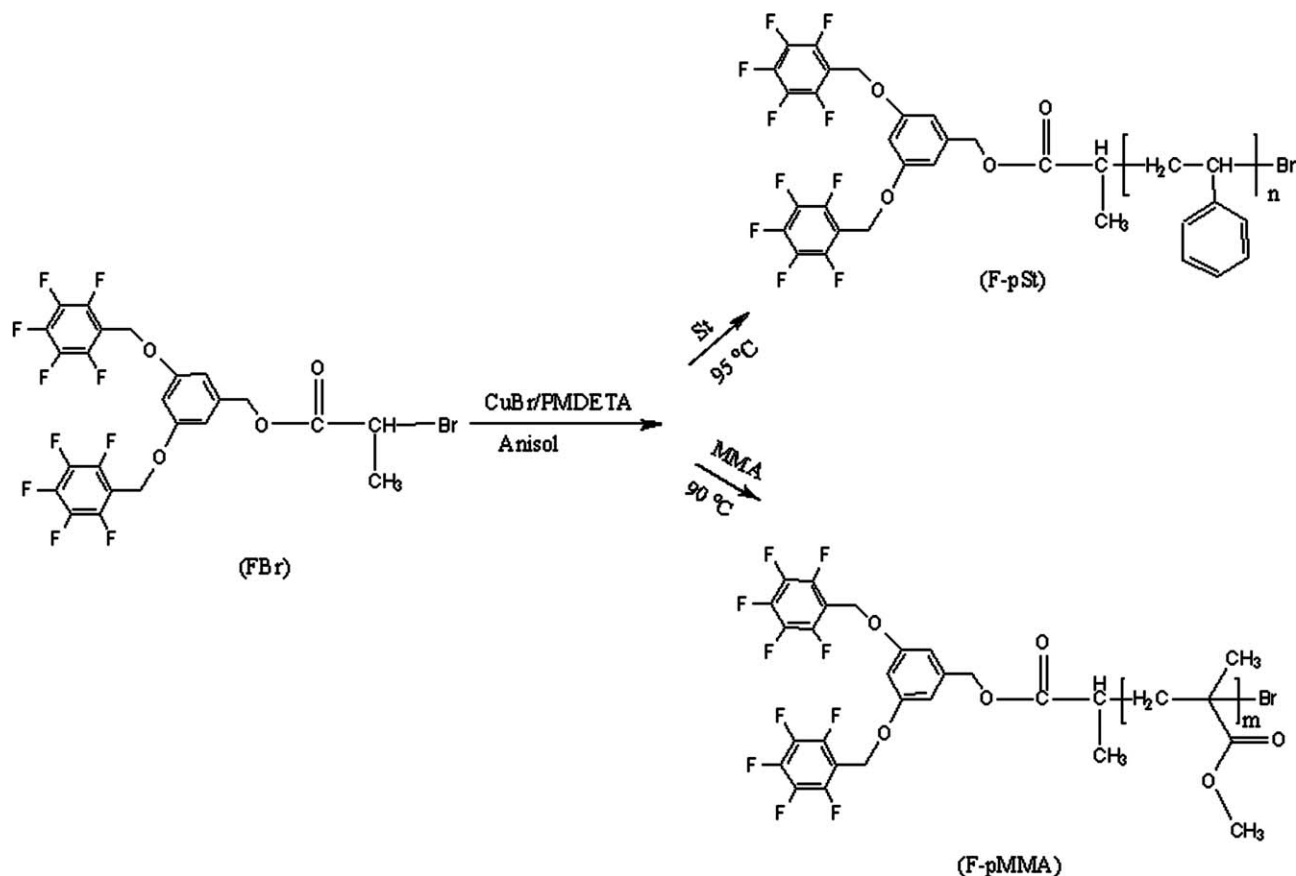
Scheme 3 Synthesis of F-pSt and F-pMMA polymers.

Run	Time (h)	$[M_0]/[I_0]$	Conv. (%)[b]	$M_{n, \text{th}}$[c]	$M_{n, \text{exp}}$[d]	M_w/M_n[d]
F-pSt0	6	200	0	–	–	–
F-pSt1	12	200	25.6	5325	8740	1.18
F-pSt2	24	200	64.4	13,395	28,800	1.09
F-pSt3	36	200	71.4	14,851	54,200	1.07
F-pSt4	48	200	83.2	17,306	67,300	1.07
F-pMMA1	3	80	63.7	5096	20,800	1.40
F-pMMA2	6	80	66.7	5336	23,000	1.35
F-pMMA3	12	80	78.7	6296	33,700	1.25
F-pMMA4	24	80	78.1	6248	35,800	1.25
F-pMMA5	36	80	81.0	6480	38,100	1.24

[a] $[I]_0 : [CuBr]_0 : [PMDETA]_0 : [Monomer]_0 = 1 : 1: 2 : 200$ in anisole at 95°C for pSt. $[I]_0 : [CuBr]_0 : [PMDETA]_0 : [Monomer]_0 = 1 : 1: 2 : 80$ in anisole at 90°C for pMMA.
[b] Determined gravimetrically.
[c] Calculated by $M_{n, \text{th}} = ([M_0]/[I_0]) \times (\text{conversion } \%) \times M_{\text{monomer}}$.
[d] Determined by means of GPC calibrated with pSt standards.

The peak observed at 4.5 ppm corresponded to CH-Br protons and spectrum indicated the presence of one *Ar*-H proton at 6.6 ppm, two *Ar*-H at 5.2 ppm, —OCH$_2$ *Ar* protons at 5.1 ppm and CH$_3$ protons at 1.7–1.9 ppm. ^{19}F-NMR spectrum showed signals at -145.1, -155.3, and -164.4 ppm assigned to *ortho*-F, *para*-F, and *meta*-F atoms in the aromatic ring respectively (Fig. 3).

ATRP, a radical process that is more tolerant to impurities, is a good method for the synthesis of polymers with well-defined compositions, architectures, and functionalities. The FBr initiator with bromine group was used to initiate the ATRP of styrene (St) and methylmethacrylate (MMA) to obtain a one-end-capped fluorinated polymer (Scheme 3). Typical results concerning the ATRP of monomers are presented in Table I.

As shown in Table I, as the conversion increased with the time, polydispersities decreased during the polymerizations. For F-pSt1 and F-pSt2 polymers, it can be said that an acceptable agreement of theoretical and experimental number-average molecular weight $M_{n, \text{th}}$, $M_{n, \text{exp}}$ and polydispersity index 1.18 and 1.09 was obtained. F-pSt3 and F-pSt4 polymers showed $M_{n, \text{exp}}$, more than three times as high as $M_{n, \text{th}}$ and a polydispersity index 1.07.

For the polymerization of styrene at the very beginning of the reaction $M_{n, \text{th}}$ and $M_{n, \text{exp}}$ were close to each other after some time the termination reactions occurred resulting much higher molecular
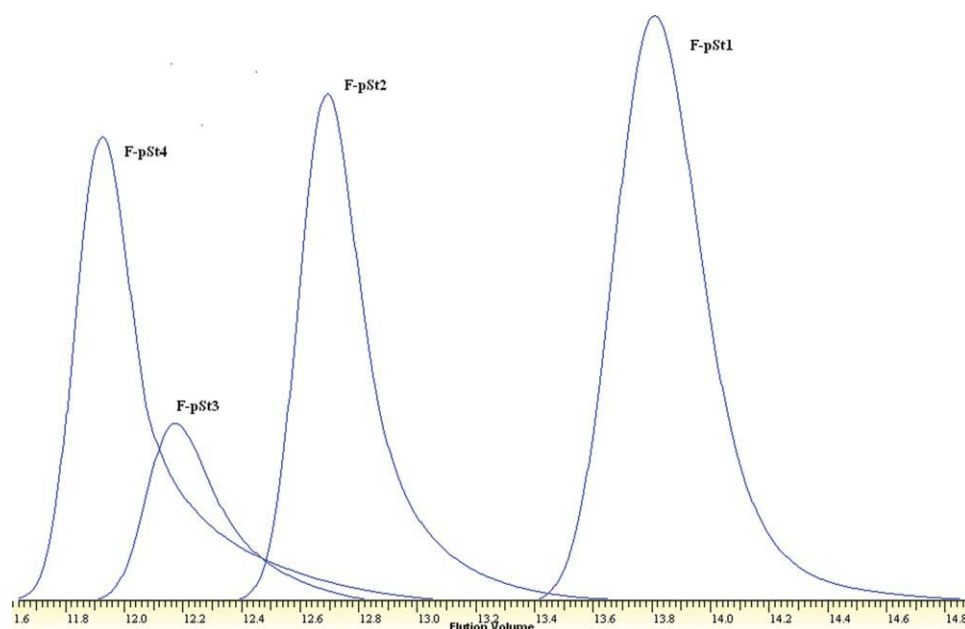

Figure 4 GPC traces of F-pSt polymers [Color figure can be viewed in the online issue, which is available at wileyonlinelibrary.com].
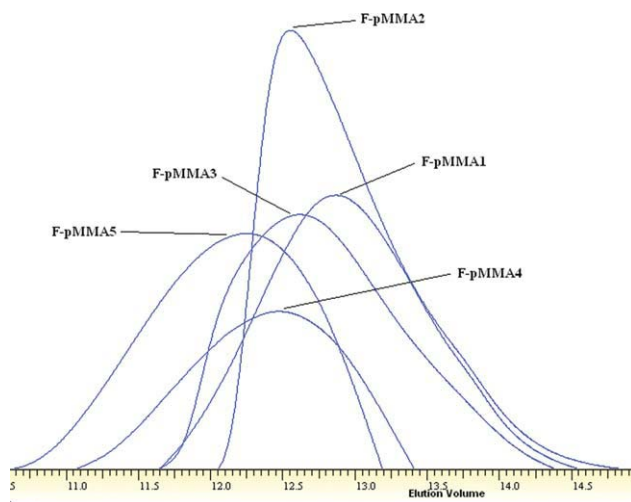
Figure 5 GPC traces of F-pMMA polymers [Color figure can be viewed in the online issue, which is available at wileyonlinelibrary.com].

weights with low polydispersities. ATRP is moderately sensitive to oxygen. The polymerization will proceed in the presence of a small amount of oxygen, because small amounts of oxygen can be scavenged by the catalyst, which is present at a much higher concentration than the growing radicals.[27] In some cases, oxygen may produce peroxides that can

actually catalyze the reaction. The polymerization of several monomers in the presence of small amounts of oxygen and Cu (I) or Cu (II) complexes has recently been reported to yield high molecular weight products with relatively low polydispersities.[27] The results appeared to be uncontrolled ones for the MMA. From the very beginning of the reaction, $M_{n,\,th}$ and $M_{n,\,exp}$ were different from each other. This could be due to low initiation efficiency of the initiator. In ATRP reactions, not all initiators are good for all monomers. For a good controlled ATRP, It is necessary to better correlate structures of the initiator with the monomer. Having more similar chemical structure of the initiator to the monomer, causes more efficient initiation. Styrene monomer have aromatic group which is more similar structure to initiator than methylmethacrylate.

It was assumed that in the absence of side reactions only a small amount of FBr initiated the polymerization, causing $M_{n,\,exp}$ of the product to be much higher than $M_{n,\,th}$ and the molecular weight distribution to be relatively narrow. According to our results, it can be said that while getting reasonable results for the styrene monomer it was not the same for methylmethacrylate with higher polydispersities. Also steric hindrance can cause the chain termination that, it could get harder to add a new
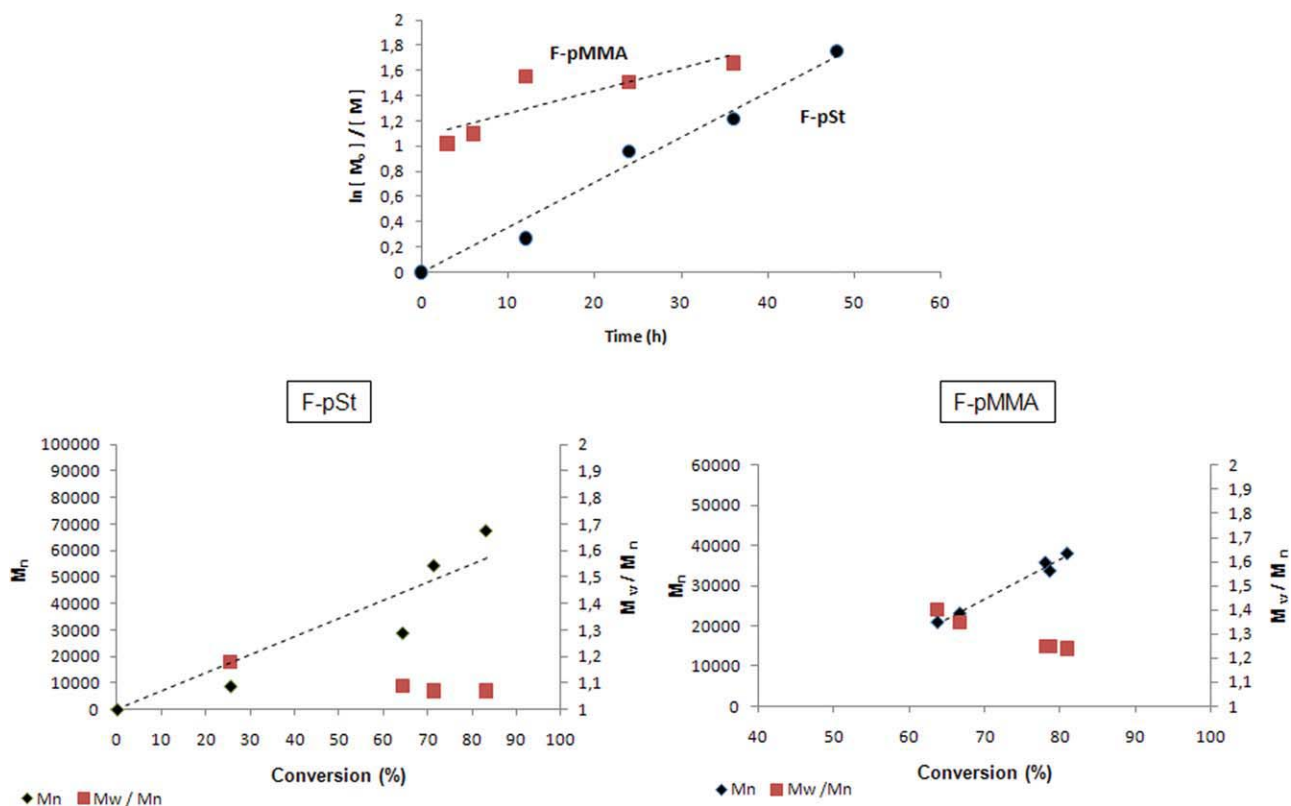

Figure 6 First-order kinetic plots for the polymerization of MMA and St using CuBr catalyst in anisole at 90 and 95°C. ■: $[M]/[I]/[Cu]/[PMDETA] = 80/1/1/2$, $[M_{MMA}]_0 = 5.61M$, ●: $[M]/[I]/[Cu]/[PMDETA] = 200/1/1/2$, $[M_{St}]_0 = 3.73M$ [Color figure can be viewed in the online issue, which is available at wileyonlinelibrary.com].
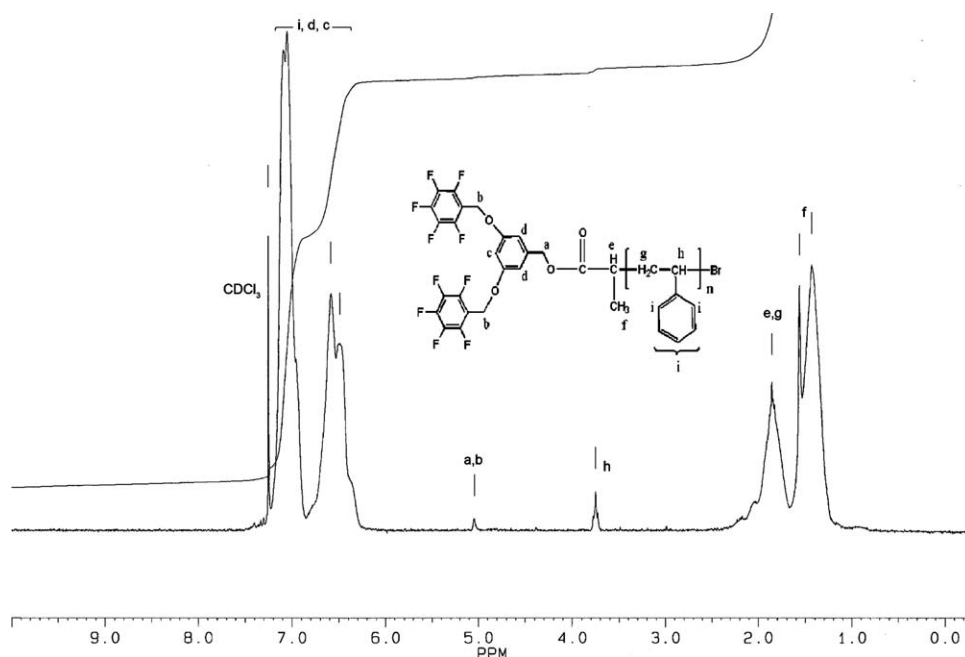
Figure 7 ^{1}H-NMR spectrum of F-pSt1 in CDCl$_3$.

monomer to the chain growed with a bulky fluorine group at the end so the chains prefered termination by combining two growing chains resulting higher molecular weights. At the very beginning of ATRP, initiation might be lower than the rate of propagation or some termination reactions occurred. This leads to the coexistence of initiation and propagation reaction and explains the tailing toward lower molecular weights in the GPC trace (Figs. 4 and 5).

For F-pMMA1, F-pMMA2, F-pMMA3, and F-pMMA4 polymers, $M_{n,\ exp}$ is more than two times higher than $M_{n,\ th}$ although the polydispersity index is still low. This can be explained by investigations of imperfections such as slow initiation, termination, transfer, and slow exchange and their effects on kinetics, molecular weight, and polydispersities of "living" chain growth polymerization.[53] During the polymerization, initiating efficiency is decreasing,
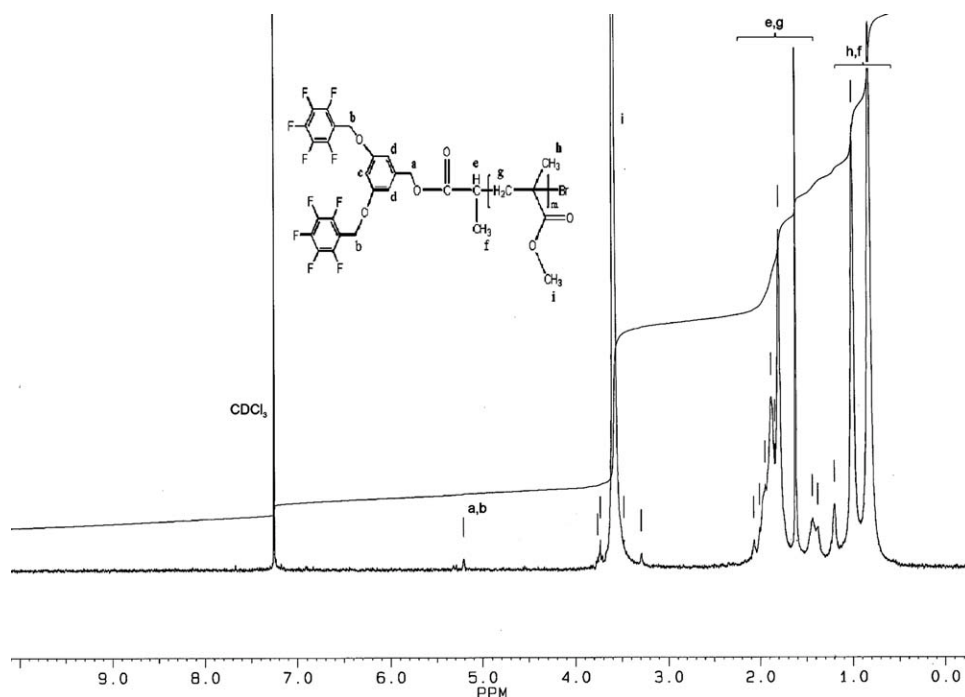

Figure 8 ^{1}H-NMR spectrum of F-pMMA1 in CDCl$_3$.

TABLE II
DSC and TGA Results for Polymers F-pSt and F-pMMA

Polymers	T_g (°C)	$T_{\%50}$ (°C)	Residue at 500°C (%)
F-pSt1	94	404	3.0
F-pSt2	97	414	1.1
F-pSt3	98	417	2.1
pSt[a]	100	416	0.0
F-pMMA1	120	376	1.6
F-pMMA2	119	377	2.1
F-pMMA3	123	377	1.2
pMMA[a]	120	366	0.0

[a] Molecular weights of pure pSt and pure pMMA were 30,230 g/mol and 30,530 g/mol, respectively.

Figure 10 DSC thermograms of F-pMMA polymers.

this could be due to some chains in polymer lost its active end during the polymerization because of the termination reactions. Very reactive initiators may produce too many radicals, which will terminate at early stages.[27] This will reduce efficiency of initiation, produce too much of the deactivator.

Table I shows the increase of monomer conversion with time, which is a basic requirement for living systems. Figure 6 shows, the semilogarithmic kinetic plot of ln ($[M]_0/[M]_t$) versus time, t, where $[M]_0$ is the initial concentration of the monomer, and $[M]_t$ is the monomer concentration at any time and also plots of M_n and polydispersity indexes (M_w/M_n) as a function of conversion. The linearity of the plot especially for the St indicates that the concentration of growing radicals is constant.

In the ^{1}H-NMR spectrum of pSt (Fig. 7), the chemical shifts at 6.2–7.2 ppm corresponded to the benzene ring protons of pSt and initiator. The complete disappearance of initiator CH-Br signals at 4.5 ppm in Figure 2 indicated that Br functions took part in initiating the pSt chain growth. At the same time, a new signal at 3.7 ppm appeared that came from Ar-CH-Br end-group protons of pSt.

The bands at 0.82, 1.00, and 1.20 ppm in the ^{1}H-NMR spectrum of pMMA (Fig. 8), represented the resonance of syndiotactic, atactic, and isotactic
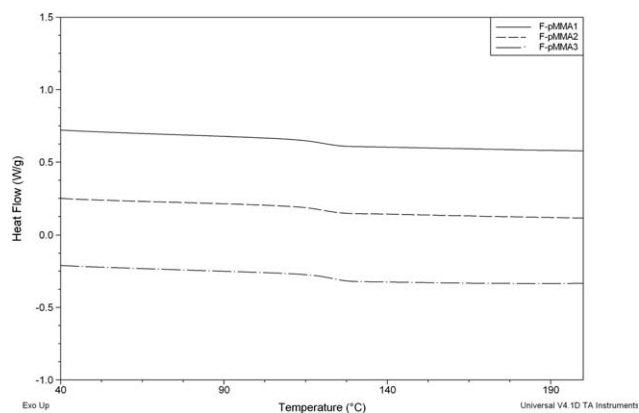
methyl groups. The methylene proton of pMMA resonances between 1.4 and 2.4 ppm. The signals observed at 3.58 ppm corresponded to the methyl of the ester group of MMA, and the peak at 5.20 ppm were assigned to –OCH$_2$ protons of FBr initiator at the end of the polymer chain.

Thermal behaviors of polymers were checked with DSC and TGA measurements. The results of thermal analysis are summarized in Table II.

The terminal fluorine group can influence the glass transition temperature at the surface region.[52,54] The terminal perfluorinated aromatic groups were to be preferentially segregated at the surface. Therefore, the lower T_g values according to pure pSt may possibly be attributed to the difference of the surface concentration of chain ends and high surface mobilities of fluorine groups (Fig. 9). As shown in Figure 10, glass transition temperatures of the obtained F-pMMA polymers were in good agreement with the T_g value of pure pMMA.

The introduction of fluorine end groups into the pSt and pMMA polymers was expected to improve their thermal stability. At 500°C, higher char yields were obtained indicating that perfluorinated aromatic group end-capped polymers exhibited better
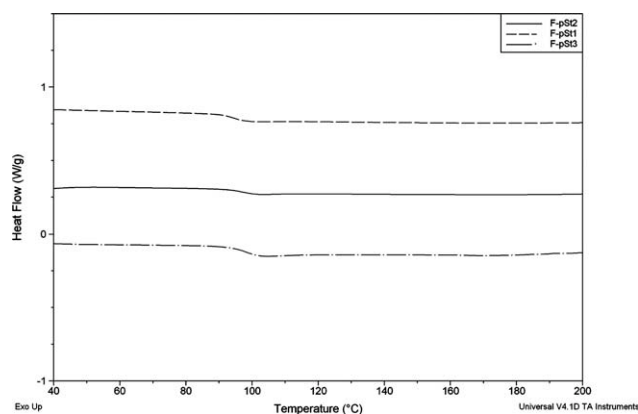

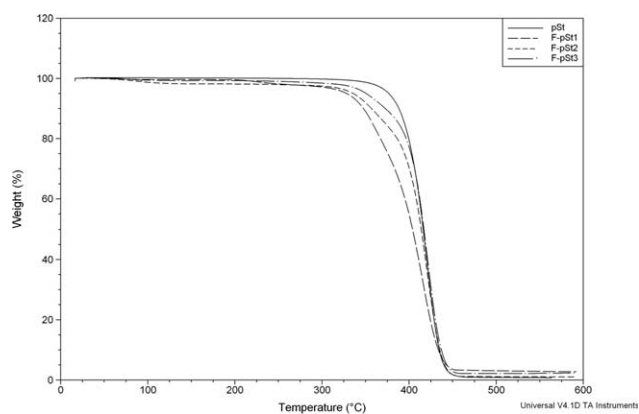**Figure 9** DSC thermograms of F-pSt polymers.

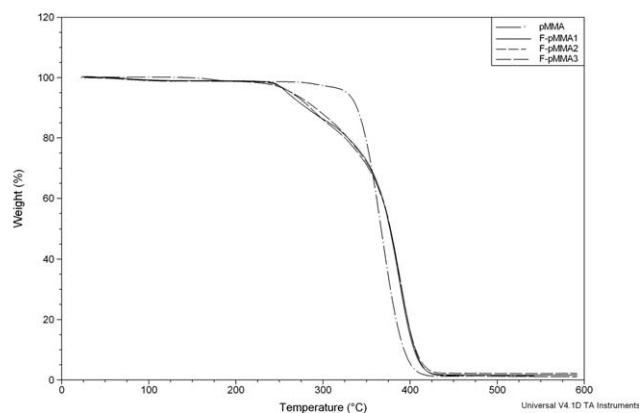**Figure 11** TGA thermograms of pSt and F-pSt polymers.

Figure 12 TGA thermograms of pMMA and F-pMMA polymers.

thermal stability than that of pure pSt and pure pMMA (Table II, Figs. 11 and 12).

Due to low surface energies and high incompatibilities of fluorine end groups, these groups are segregated significantly at the polymer surfaces or air–polymer interfaces.[55–59] Appreciable surface and interfacial segregation of fluorine end groups is also observed in almost all the blend systems composed of polymers chain-end-functionalized with fluorine group(s) and nonfluorine-polymers.[60–64] Even small amounts of fluorine end groups significantly reduce the surface energy of polymer and blend surfaces. The extent of such surface segregation might be quantitatively evaluated by analytical methods such as contact angle measurements. To investigate the
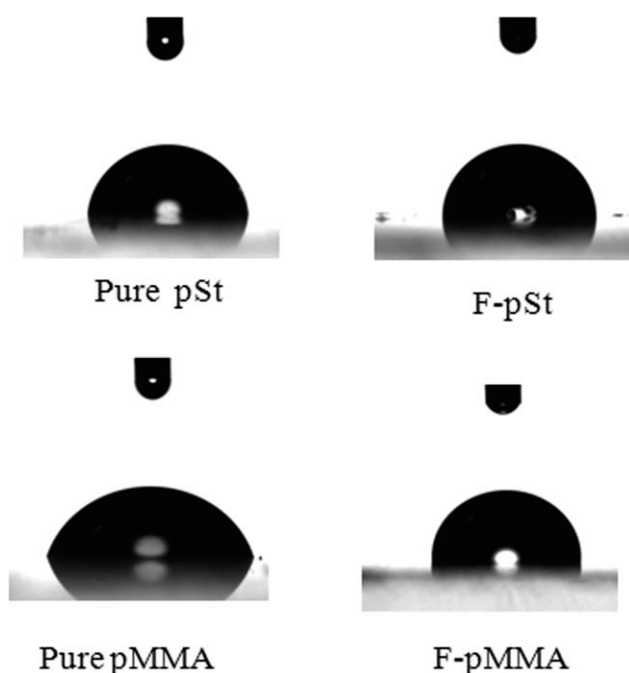

Figure 13 Photographs of 5 μL drops of water on nonfluorinated and fluorinated polymer samples.

TABLE III
Surface Properties of Spin Cast Polymer Films

Material	Water contact angle (°)	Ethylene glycol contact angle (°)	Geometric mean equation surface energy (mN/m)		
			$\gamma_s^{p,a}$	$\gamma_s^{d,a}$	γ_s^a
Pure pSt	90.4	71.3	6.6	14.4	21.1
F-pSt1	94.6	72.8	3.7	17.7	21.4
F-pSt2	97.6	75.2	2.6	18.3	20.9
F-pSt3	96.5	76.0	3.7	15.8	19.5
Pure pMMA	73.6	54.2	16.5	14.2	30.8
F-pMMA1	85.7	64.1	7.6	17.5	25.1
F-pMMA2	84.8	67.6	10.7	12.3	23.0
F-pMMA3	90.8	72.1	6.7	13.9	20.1

[a] γ_s^d: dispersion component; γ_s^p: polar (nondispersion) component; γ_s: surface energy.

effect of the incorporated perfluorinated aromatic group on the surface property of polymers, contact angle measurements were performed with deionized water and ethylene glycol as wetting agent.

F-pSt and F-pMMA films were spin-coated from solutions onto glasses. Afterward, contact angles of water and ethylene glycol were measured to determine the relative wettabilities of the film surfaces. Also, surface free energy of the films were calculated from the average contact angles. Owens-Wendt geometric mean with the two-liquid method[52,54] was applied. Figure 13 shows photographs of water drops on the polymer film samples and Table III summarizes the results.

Contact angle measurements indicate that the surface of F-pSt and F-pMMA polymer films have more hydrophobic character, when compared with fluorine-free pSt and pMMA. Contact angle values elevate when the molecular weight of the polymer increased as a result of having more chains with fluorinated ends.

Spin coated film of pure pSt showed a contact value of 90° (for water) and 71° (for ethylene glycol) while fluorinated pSt (F-pSt) films had contact angle values between 94°–96° (for water) and 72°–76° (for ethylene glycol), also fluorinated pMMA (F-pMMA) films showed higher contact angle values between 85°–90° (for water) and 64°–72° (for ethylene glycol) in comparison with pure pMMA film having 73° (for water) and 54° (for ethylene glycol) contact angle value. Also, the surface energies of the fluorinated pSt and pMMA are lower than their fluorine free analogues.

CONCLUSIONS

A new ATRP initiator, 3,5-bis(perfluorobenzyloxy)-benzyl 2-bromopropanoate (FBr) having perfluorinated aromatic group was synthesized and used to

perform ATRP of styrene (St) and methylmethacrylate in the presence of CuBr/PMDETA. The structures of the initiator and polymers were thoroughly characterized and confirmed using NMR spectroscopy. ATRP of St and MMA afforded perfluorinated aromatic group-terminated pSt and pMMA with narrow molecular weight distribution. A linear relationships between both $\ln[M]_0/[M]$ vs. time and molecular weight vs. conversion indicated controlled/living polymerization of St using FBr as ATRP initiator. The DSC results correlate well with the results of pure pSt and pMMA polymers. Introducing the fluorinated groups into the polymer gave higher residue in the TGA analysis. Contact angle measurements indicated that the surface wettability of the obtained films decreased significantly. As a further study, to use many unique advantages contributed by the fluorine group, this type of perfluorinated aromatic group containing monomers can be polymerized to form block copolymers in which more fluorine groups are incorporated.

References

1. Delucchi, M.; Turri, S.; Barbucci, A.; Bassi, M.; Novelli, S.; Cerisola, G. J Polym Sci Part B: Polym Phys 2002, 40, 52.
2. Wang, J. G.; Mao, G. P.; Ober, C. K.; Kramer, E. J. Macromolecules 1997, 30, 1906.
3. Honeychuck, R. V.; Ho, T.; Wynne, K. J.; Nissan, R. A. Chem Mater 1993, 5, 1299.
4. Chapman, T. M.; Marra, K. G. Macromolecules 1995, 28, 2081.
5. Yoon, S. C.; Ratner, B. D. Macromolecules 1986, 19, 1068.
6. Tang, Y. W.; Santerre, J. P.; Labow, R. S.; Taylor, D. G. J Appl Polym Sci 1996, 62, 1133.
7. Park, I. J.; Lee, S.-B.; Choi, C. K. J Appl Polym Sci 1994, 54, 1449.
8. Kano, Y.; Akiyama, S. Polymer 1996, 37, 4497.
9. Valade, D.; Boschet, F.; Ameduri, B. Macromolecules 2009, 42, 7689.
10. Affrossman, S.; Bertrand, P.; Hartshorne, M.; Kiff, T.; Leonard, D.; Pethrick, R. A.; Richards, R. W. Macromolecules 1996, 29, 5432.
11. Schaub, T. F.; Kellog, G. J.; Mayes, A. M.; Kulasekere, R.; Ankner, J. F.; Kaiser, H. Macromolecules 1996, 29, 3982.
12. Tang, C.; Liu, W. J Appl Polym Sci 2010, 117, 1859.
13. Ameduri, B. Macromolecules 2010, 43, 10163.
14. Imae, T. J Colloid Interface Sci 2003, 8, 307.
15. Iyengar, D. R.; Perutz, S. M.; Dai, C.-A.; Ober, C. K.; Kramer, E. J. Macromolecules 1996, 29, 1229.
16. Lou, L.; Koike, K.; Okamoto Y. J Polym Sci Part A: Polym Chem 2010, 48, 4938.
17. Dimitrov, I.; Jankova, K; Hvilsted, S. J Polym Sci Part A: Polym Chem 2010, 46, 7827.
18. Malshe, V. C.; Sangaj, N. S. Prog Org Coat 2005, 53, 207.
19. Matyjaszewski, K.; Davis, T. P. Handbook of Radical Polymerization; Wiley: New York, 2002.
20. Wang, J.; Matyjaszewski, K. J Am Chem Soc 1995, 117, 5614.
21. Kato, M.; Kamigaito, M.; Sawamoto, M.; Higashimura, T. Macromolecules 1995, 28, 1721.
22. Georges, M.; Veregin, R.; Kazmaier, P.; Hamer, G. Macromolecules 1993, 26, 2988.
23. Wang, J. S.; Matyjaszewski, K. Macromolecules 1995, 28, 7901.
24. Matyjaszewski, K.; Jo, S. M.; Paik, H.; Gaynor, S. Macromolecules 1997, 30, 6398.
25. Matyjaszewski, K.; Miller, P.; Shukla, N.; Immaraporn, B.; Gelman, A.; Luokala, B.; Siclovan, T.; Kickelbick, G.; Vallant, Th.; Hoffmann, H.; Pakula, T. Macromolecules 1999, 32, 8716.
26. Save, M.; Weavers, J.; Armes, S. Macromolecules 2002, 35, 1152.
27. Matyjaszewski, K., Xia, J. Chem Rev 2001, 101, 2921.
28. Kamigaito, M.; Ando, T.; Sawamoto, M. Chem Rev 2001, 101, 3689.
29. Percec, V.; Barboiu, B. Macromolecules 1995, 28, 7970.
30. Haddleton, D.; Crossman, M.; Dana, B.; Duncalf, D.; Heming, A.; Kukulj, D.; Shooter, A. Macromolecules 1999, 32, 2110.
31. Haddleton, D.; Jasieczek, Ch.; Hannon, M.; Shooter, A. Macromolecules 1997, 30, 2190.
32. Haddleton, D.; Perrier, S.; Bon, S. Macromolecules 2000, 33, 8246.
33. Moineau, G.; Granel, C.; Dubois, Ph.; Jérôme, R.; Teyssié, P. Macromolecules 1998, 31, 542.
34. Moineau, G.; Dubois, Ph.; Jérôme, R.; Senninger, T.; Teyssié, P. Macromolecules 1998, 31, 545.
35. Nishikawa, T.; Ando, T.; Kamigaito, M.; Sawamoto, M. Macromolecules 1997, 30, 2244.
36. Lecomte, Ph.; Drapier, I.; Dubois, Ph.; Teyssié, Ph.; Jérôme, R. Macromolecules 1997, 30, 7631.
37. Granel, C.; Dubois, Ph.; Jérôme, R.; Teyssié, Ph. Macromolecules 1996, 29, 8576.
38. Ando, T.; Kamigaito, M.; Sawamoto, M. Macromolecules 1997, 30, 4507.
39. Matyjaszewski, K.; Wei, M.; Xia, J.; McDermott, N. E. Macromolecules 1997, 30, 8161.
40. Zhu, Sh.; Yan, De.; Zhang, G.; Li, M. Macromol Chem Phys 2000, 201, 2666.
41. Gibson, V. C.; O'Reilly, R. K. Polym Prepr 2004, 45, 680.
42. Wang, X.-S.; Lascelles, S. F.; Jackson, R. A.; Armes, S. P. Chem Commun 1999, 18, 1817.
43. Robinson, K. L.; De Paz-Banez, M. V.; Wang, X. S.; Armes, S. P. Macromolecules 2001, 34, 5799.
44. Koh, K.; Sugiyama, S.; Morinaga, T.; Ohno, K.; Tsujii, Y.; Fukuda, T. Macromolecules 2005, 38, 1264.
45. Destarac, M.; Matyjaszewski, K.; Silverman, E.; Ameduri, B.; Boutervin, B. Macromolecules 2000, 33, 4613.
46. Shi, Z.; Holdcroft, S. Macromolecules 2004, 37, 2084.
47. Perrier, S.; Jackson, S. J.; Haddleton, D. M.; Ameduri, B.; Boutevin, B. Macromolecules 2003, 36, 9042.
48. Feiring, A. E.; Wonchoba, E. R.; Davidson, F.; Percec, V.; Barboiu, B. J Polym Sci Part A: Polym Chem 2000, 38, 3313.
49. Perrier, S.; Lackson, S. G.; Haddleton, D. M.; Ameduri, B.; Boutevin, B. Tetrahedron 2002, 58, 4053.
50. Li, H.; Zhang, Y. M.; Zhang, H.; Xue, M. Z.; Liu, Y. G. J Polym Sci Part A: Polym Chem 2006, 44, 3853.
51. Hirao, A.; Sugiyama, K.; Yokoyama, H. Prog Polym Sci 2007, 32, 1393.
52. Owens, D. K.; Wendt, R. C. J Appl Polym Sci 1969, 13, 1741.
53. Matyjaszewski, K. J Phys Organ Chem 1995, 8, 197.
54. Kinloch, A. J. Adhesion and Adhesives; Chapman and Hall: London, 1987.
55. Hunt, M. O., Jr.; Belu, A. M.; Linton, R. W.; DeSimone, J. M. Macromolecules 1993, 26, 4854.
56. Jiang, X.; Yang, C. Z.; Tanaka, K.; Takahara, A.; Kajiyama, T. Phys Lett A 2001, 281, 363.
57. Sugiyama, K.; Hirao, A.; Nakahama, S. Macromol Chem Phys 1996, 197, 3149.
58. El-Shehawy, A. A.; Yokoyama, H.; Sugiyama, K.; Hirao, A. Macromolecules 2005, 38, 8285.

59. McLain, S. J.; Sauer, B. B.; Firment, L. E. Macromolecules 1996, 29, 8211.

60. Affrossman, S.; Hartshorne, J. M.; Kiff, T.; Pethrick, R. A.; Richards, R. W. Macromolecules 1994, 27, 1588.

61. Schaub, T. F.; Kellogg, G. J.; Mayes, A. M.; Kulasekere, R.; Ankner, J. F.; Kaiser, H. Macromolecules 1996, 29, 3982.

62. Affrossman, S.; Bertrand, P.; Hartshorne, M.; Kiff, T.; Leonard, D.; Pethrick, R. A. Macromolecules 1996, 29, 5432.

63. Hopkinson, I.; Kiff, F. T.; Richards, R. W.; Bucknall, D. G.; Clough, A. S. Polymer 1997, 38, 87.

64. O'Rourke Muisener, P. A. V.; Jalbert, C. A.; Yuan, C.; Baetzold, J.; Mason, R.; Wong, D. Macromolecules 2003, 36, 2956.